"UV-SI" UV-B component of sunlight stimulates photosynthesis and flavonoid accumulation in variegated *Plectranthus coleoides* leaves depending on background light

MARIJA VIDOVIĆ[1], FILIS MORINA[1], SONJA MILIĆ[1], BERND ZECHMANN[3], ANDREAS ALBERT[2], JANA BARBRO WINKLER[2], SONJA VELJOVIĆ JOVANOVIĆ[1*]

[1]Institute for Multidisciplinary Research, University of Belgrade, Kneza Viseslava 1, 11000, Belgrade, Serbia, [2]Research Unit Environmental Simulation, Helmholtz Zentrum München, Ingolstädter Landstr. 1, 85764 Neuherberg, Germany and [3]Baylor University, Center for Microscopy and Imaging, One Bear Place #97046, Waco, TX 76798-7046, USA

Running title: UV-B radiation response in variegated *P. coleoides*

Correspondence: S. Veljović Jovanović, e-mail: sonjavel@imsi.rs

This article has been accepted for publication and undergone full peer review but has not been through the copyediting, typesetting, pagination and proofreading process, which may lead to differences between this version and the Version of Record. Please cite this article as doi: 10.1111/pce.12471

Abstract

We used variegated *Plectranthus coleoides* as a model plant with the aim of clarifying whether the effects of realistic UV-B doses on phenolic metabolism in leaves are mediated by photosynthesis. Plants were exposed to UV-B radiation (0.90 W m^{-2}) combined with two PAR intensities (395 and 1350 μmol m^{-2} s^{-1}, LL and HL) for nine days in sun simulators. Our study indicates that UV-B component of sunlight stimulates CO_2 assimilation and stomatal conductance, depending on background light. UV-B-specific induction of apigenin and cyanidin glycosides was observed in both green and white tissues. However, all the other phenolic subclasses were up to four times more abundant in green leaf tissue. Caffeic and rosmarinic acids, catechin and epicatechin, which are endogenous peroxidase substrates, were depleted at HL in green tissue. This was correlated with increased peroxidase and ascorbate peroxidase activities and increased ascorbate content. The UV-B supplement to HL attenuated antioxidative metabolism and partly recovered the phenolic pool indicating stimulation of the phenylpropanoid pathway. In summary, we propose that *ortho*-dihydroxy phenolics are involved in antioxidative defence in chlorophyllous tissue upon light excess, while apigenin and cyanidin in white tissue have preferentially UV-screening function.

Keywords

Ascorbate, chloroplast ultrastructure, cyanidin, flavonoids, high light, photosynthesis, UV-B radiation, variegated plants.

Introduction

Plants are inevitably exposed to fluctuating light intensities of photosynthetically active radiation (PAR, 400 - 700 nm) and ultraviolet radiation (UV, 280 - 400 nm) in their natural environment. In addition to light quantity, plants monitor the quality, periodicity and direction of light and use the information as an environmental signal to regulate growth and development (reviewed in Caldwell *et al.* 2007; Jiao, Lau & Deng 2007). Persistently high PAR, however, can overcome the capacity of the photosynthetic assimilation and energy dissipation processes and provoke generation of reactive oxygen species (ROS) (Asada 2006; Foyer & Shigeoka 2011; Fischer, Hideg & Krieger-Liszkay 2013). In addition, high fluence rates of UV-B radiation (280-315 nm) are also detrimental for plants, inducing DNA damage, oxidative stress and photosynthetic inhibition (Hideg &Vass 1996; Jansen, Gaba & Greenberg 1998; Brosché & Strid 2003). Although numerous studies have shown that photosynthesis is susceptible to UV-B radiation (Teramura & Sullivan 1994; Jansen *et al*., 2010; Lidon *et al*. 2012), plants rarely show signs of damage even though they are continuously exposed to natural UV-B radiation (Hideg, Jansen & Strid 2013). Reports of the effects of UV-B radiation on photosynthetic gas exchange parameters are inconsistent, which may be explained by various experimental conditions, different UV-B/PAR ratios, time of exposure, and species/cultivar-specific sensitivity to UV-B radiation and previous acclimation periods (reviewed in Kakani *et al.* 2003; Lidon *et al.* 2012; Hideg, Jansen & Strid 2013). Moreover, the results related to stomatal response to UV-B radiation are still controversial, e.g., depending on the metabolic state of the plant or acclimation (Jansen & van den Noort 2000; Kakani *et al.* 2003; Lidon *et al.* 2012). Only recent studies exploiting realistic light conditions noted that low, ecologically relevant UV-B doses provide a regulatory signal via rapid activation of UVR8, a specific UV-B receptor (Jenkins 2009; Heijde & Ulm 2012). Accordingly, it was reported that relevant ambient UV-B doses (under

field conditions) have minimal effects on photosynthesis and plant biomass (Ballaré *et al.* 2011; Hideg, Jansen & Strid 2013).

The main components of the acclimation response to natural UV-B doses are UV-B absorbing flavonoids and other phenolics. It has been shown that the induction of flavonoid biosynthesis is regulated through UVR8 activation of chalcone synthase (Jenkins 2009; Heijde & Ulm 2012). Depending on their location in the leaf and their structure, they can act as UV-B screeners (epidermis) and antioxidants (e.g., mesophyll) (Rice-Evans, Miller & Papanga 1996; Neill *et al.* 2002; Agati *et al*. 2009; Agati & Tattini 2010). Moreover, hydroxycinnamic acids, such as caffeic, *p*-coumaric and their derivatives (e.g., rosmarinic and chlorogenic acids), and flavonoids (catechin, quercetin) are endogenous substrates for class III peroxidases (PODs) (Chan, Galati & O'Brien 1999; Takahama 2004).

The ascorbate/phenolics/peroxidase system has an important H_2O_2 scavenging function in the vacuoles and apoplast (Takahama & Oniki 1997). In addition, ascorbate (Asc) can scavenge H_2O_2 in reactions catalysed by ascorbate peroxidase (APX) (Asada 2006). It has been shown that UV-B radiation provokes the up-regulation of antioxidative metabolism (Brosché *et al*, 2002; Brown *et al.*, 2005; Xu, Natarajan & Sullivan, 2008; Jansen, Hideg & Lidon 2012; Hideg, Jansen & Strid 2013). Furthermore, high light intensity enhances the levels of antioxidants, particularly Asc and APX (Fryer *et al*. 2003; Bartoli *et al*. 2006, Szechyńska-Hebda & Karpiński 2013).

Considering that under field conditions both high PAR and UV-B radiation affect plants, the aim of our study was to distinguish between the UV-B- and PAR-specific responses of photosynthesis, phenolics and antioxidants. We exploited green-white variegated *Plectranthus coleoides* (Swedish ivy) leaves as a suitable plant system to clarify whether the specific effects of UV-B radiation are mediated by photosynthesis. Furthermore,

we investigated whether UV-B radiation supplemented to high light has beneficial effects in both "source" (photosynthetically active) and "sink" (non-photosynthetically active) tissues.

Materials and methods

Plant material and experimental conditions

Green-white variegated *Plectranthus coleoides* plants (Swedish ivy) were obtained from a nursery in Belgrade and placed in the greenhouse of the Helmholtz Zentrum München (Neuherberg, Germany). The greenhouse had an UV-transparent glass cover where approximately 50% was in the visible and UV-A part of the solar downwelling radiation, and approximately 20% of the UV-B radiation was reached at the plant level compared to outside conditions.

The nine-day experiment was conducted in the sun simulators of the Helmholtz Zentrum München (Neuherberg, Germany). The sun simulators provided an irradiance spectrum close to natural solar radiation (Supporting Information, Fig. S1) by the use of a combination of metal halide lamps (HQI/D, 400 W, Osram, Munich, Germany), quartz halogen lamps (Halostar, 300 W and 500 W, Osram, Munich, Germany), blue fluorescent (TLD 18, 36 W, Philips, Amsterdam, The Netherlands) and UV-B fluorescent (TL12, 40 W, Philips, Amsterdam, The Netherlands) tubes. Excess infrared radiation was reduced by a layer of water, and wavelengths below 280 nm were efficiently blocked using selected borosilicate and lime glass filters. A suitable combination of these glasses allowed us to simulate the different UV-B scenarios (Thiel *et al.* 1996, Döhring *et al.* 1996). The photoperiod was 12 h with day and night temperatures of 25 and 18 ºC and relative humidities of 55% and 80%, respectively; the plants were watered daily. The natural diurnal variations of the solar irradiance were obtained by using specific groups of lamps and by changing the climate parameters gradually during two hours at the beginning and at the end

of the day. For the acclimatisation period of six days, PAR intensity was maintained at 395 μmol m^{-2} s^{-1} (corresponding to the greenhouse conditions) without UV-B radiation. At the start of the experiment, the PAR intensity was 395 μmol m^{-2} s^{-1} in the LL experiment in the first sun simulator (resulting in 14.2 mol m^{-2} PAR per day) and was raised to 1350 μmol m^{-2} s^{-1} PAR in the HL experiment in the second simulator (resulting 48.8 mol m^{-2} PAR per day). Additionally, UV-B radiation (0.90 W m^{-2}) was applied one hour after the onset of PAR in one separated compartment of each sun simulator (LL and HL), which resulted in a 29.3 kJ m^{-2} daily UV-B dose or a 7.0 kJ m^{-2} daily biologically effective UV-B dose (calculated using Green et al. (1974) according to the measurements of Caldwell (1971) normalised at 300 nm). UV-B treatments started one day after the treatments without UV-B radiation to ensure that ecophysiological measurements were performed at the same time of the day as the treatment. In summary, four different radiation regimes were applied: (1) LL; (2) LL+ UV-B; (3) HL and (4) HL+UV-B (for detailed radiation conditions see Table 1). During exposure, the PAR, UV-A and UV-B irradiances were continuously monitored. Spectroradiometric measurements were performed using a double monochromator system TDM300 (Bentham, Reading, England). The horizontal variation of radiance values was less than 10% during and between the experiments. The irradiation regime, HL+UV-B, can be compared to sunny spring conditions in mid-northern latitudes where the sun is at approximately 40 degrees elevation and the total ozone column is approximately 300 DU (Dobson units), corresponding to an ozone column thickness of 3 mm.

Table 1.

Leaves were harvested on the last day of the experiment beginning at 14:00 hours. For the biochemical analysis, up to six mature leaves from each plant per group were pooled,

immediately frozen in liquid nitrogen and stored at −80 °C. In total, four groups of plants (four to five plants per group) were used in the HL treatments and two groups (five plants per group) in the LL treatments.

Chlorophyll fluorescence and gas exchange measurements

All chlorophyll fluorescence measurements were done daily on green leaf part. Chlorophyll fluorescence was measured by miniPAM chlorophyll fluorometer equipped with light and temperature-sensing leaf clip 2030-B (Heinz Walz GmbH, Effeltrich, Germany). The minimal fluorescence (F_0) and maximal fluorescence (F_m) were measured in dark-adapted leaves in the early morning and the photochemical yield of open PS II (variable fluorescence F_v) was calculated as F_v / F_m ($F_v = F_m - F_0$), reflecting the maximal photosynthetic efficiency of PS II. F_m was determined by applying a 1 s saturating flash of white light (4500 μmol m^{-2} s^{-1}). The maximal fluorescence (F_m') and fluorescence (F) in light-adapted leaves were measured at noon and the PS II efficiency: ($F_m' - F$) / F_m' was estimated as according to Baker (2008). Non-photochemical quenching (NPQ) was calculated according to Stern-Volmer equation NPQ = ($F_m - F_m'$) / F_m' (Bilger & Björkman 1990). Fluorescence parameters of individual plant are mean values of three leaves.

CO_2 assimilation rate (A), stomatal conductance (g_s), internal CO_2 concentration (c_i), and chlorophyll fluorescence were recorded on the first and on the ninth day of the experiment using the portable gas exchange and fluorescence system GFS-3000 equipped with the LED-Array/PAM-Fluorometer 3055-FL (Heinz Walz GmbH, Effeltrich, Germany). Gas exchange was measured at the respective PAR levels (395 and 1350 μmol m^{-2} s^{-1}). The leaf chamber environment was adjusted to experimental conditions (CO_2 concentration: 385 ppm, cuvette temperature: 25 ºC, relative humidity: 55%). The air flow rate was 700 μmol s^{-}

[1]. All measurements were performed between 11:00 – 14:00 CET on the first and the last day of the experiment.

Photosynthetic pigment determination

The same green areas of leaves as were used in gas exchange measurements were cut under the experimental light conditions, immediately frozen in liquid nitrogen and extracted with N, N, dimethylformamide (DMF). The pigments (carotenoids and chlorophyll *a* and *b*) were separated and quantified by diode-array HPLC (Waters Corp., Milford, Massachusetts, USA) as described by Wildi & Lütz (1996). The de-epoxidation index (Di) was expressed as a percent value of (0.5 x A + Z) of (V + A + Z), where A is antheraxanthin, Z is zeaxanthin, and V is violaxanthin.

Transmission electron microscopy (TEM)

Chloroplast ultrastructure in HL experiment was investigated using Philips CM 10 TEM. Small pieces from white and green leaf areas from at least three different plants per group (HL and HL+UV-B) were cut and specimen were treated according to Heyneke *et al.* (2013). Ultrathin sections (80 nm) were cut with a Reichert Ultracut S ultramicrotome (Leica Microsystems, Vienna, Austria) and stained with lead citrate and uranyl acetate. Micrographs of randomly photographed sections of the mesophyll (altogether 20 chloroplasts in HL and in HL+UV-B) were digitized, and chloroplast fine structures (thylakoids, starch, and plastoglobuli) were analyzed using the software package Optimas 6.5.1 (BioScan Corp.).

Phenolic analysis

Green and white leaf portions of *P. coleoides* were rapidly ground with a mortar and pestle to a fine powder, extracted in methanol containing 0.1% HCl, incubated for 50 min on ice in the dark and centrifuged for 10 min at 16 000 g at 4 ºC. Supernatants (600 µl) were mixed with

187 ddH_2O (400 µl) and chloroform (600 µl) (to remove hydrophobic, interfering compounds)
188 and shaken for 45 min at 4 ºC in the dark. Afterwards, the samples were centrifuged for 5 min
189 at 16 000 g and 4 ºC, and the upper water layer was split in two halves: the first half was used
190 for glycoside determination, and the second half was hydrolysed in 2 M HCl during
191 incubation at 85 ºC for 40 min, according to the modified procedure of Hertog, Hollman &
192 Venem (1992) for the determination of aglycones. Finally, all extracts were flushed with
193 nitrogen and maintained at –80 ºC until further analysis.
194 For HPLC analysis, samples were loaded onto 5.0 µm, 250 x 4.6 mm Luna C18 (2)
195 reversed-phase column (Phenomenex Ltd. Torrance, CA, USA) using a Shimadzu LC-20AB
196 Prominence liquid chromatograph (Shimadzu, Kyoto, Japan). Phenolic compounds were
197 separated at a flow rate of 1 ml min^{-1} with a mixture of solvent A (acetonitrile) and solvent B
198 (acetic acid/acetonitrile/phosphoric acid/water: 10.0/5.0/0.1/84.9, v/v/v/v) at 25 °C. The
199 following elution procedure was used to achieve separation of a wide range of phenolics: 0-5
200 min, 100% solution B (isocratic step); 5-25 min, 100-80% solution B (linear gradient); 25-35
201 min, 80-60% solution B (linear gradient); 35-40 min, 60-100% solution B (linear gradient).
202 The phenolics were analysed by SPD-M20A diode array Prominence and RF-10-AXL
203 fluorescence detector (Shimadzu, Kyoto, Japan). Chromatograms were recorded at different
204 wavelengths depending on the characteristic maximum absorbance of the selected phenolics:
205 520 nm for anthocyanins, 340 nm for flavones, 320 nm for hydroxycinnamic acids and their
206 derivatives, and 280 nm for catechins, hydroxybenzoic acids and their derivatives. Individual
207 phenolics were identified by comparing the absorption spectra to authentic standards and by
208 spiking with standards; the phenolics were quantified by peak area using Shimadzu LC
209 Solution software (Shimadzu, Kyoto, Japan).
210
211 ***Measurements of peroxidases activities and protein carbonylation level***

For extraction of peroxidase (POD, EC 1.11.1.7) frozen leaf tissues (white and green) were homogenized in liquid nitrogen and extracted with 100 mM potassium phosphate buffer (pH 7.2) with 1mM EDTA, 0.1% (v/v) Triton X-100, 5% of insoluble polyvinylpyrrolidine (PVP) and 5% protease inhibitor cocktail (Sigma). The same extraction buffer was used for ascorbate peroxidase (APX, E.C, 1.11.1.11) extraction with addition of 10 mM Asc. Following centrifugation at 10 000 g for 10 min at 4 ºC, supernatants were used for measuring enzymatic activities and determination of carbonylated protein level.

POD activity was measured as absorbance increase at 470 nm using 20 mM guaiacol ($\varepsilon = 26.6\ mM^{-1}\ cm^{-1}$) as hydrogen donor in 100 mM potassium phosphate buffer (pH 6.5) with 1.3 mM H_2O_2 and aliquot of the extract diluted 30 times. The activity of APX was measured as an initial absorbance decrease at 290 nm ($\varepsilon = 2.8\ mM^{-1}\ cm^{-1}$) in a reaction mixture consisting of 50 mM potassium phosphate buffer (pH 7.2) with 1 mM EDTA, 0.3 mM ascorbate (Asc), 0.2 mM H_2O_2 and extract diluted 20 times (modified from Nakano & Asada 1981). Control rates obtained in the absence of extracts were subtracted. The level of protein carbonylation was determined spectrophotometrically as described by Morina *et al.* (2010). The protein contents in the samples were determined according to Bradford (1976). All spectrophotometric measurements were performed in triplicates at 25 °C using a temperature-controlled spectrophotometer (Shimadzu, UV-160, Kyoto, Japan).

Ascorbate determination

Frozen green and white leaf tissues were extracted in 1.5% of *meta*-phosphoric acid containing 1mM EDTA and centrifuged at 16 000 g for 8 min at 4 °C (Tausz, Kranner & Grill 1996). For reduced Asc determination the obtained supernatants were immediately loaded onto a reversed phase column (CC 250/4.6 Nucleosil 100-5 C18, Macherey-Nagel, Germany). A gradient elution was established with 80 mM potassium phosphate buffer, pH

6.5 (solvent A) and methanol (solvent B): 0-15 min, 2.5-5.0 % solution B (linear gradient) at a flow rate of 0.8 ml min^{-1}, at 25 °C. Peak of reduced Asc was detected at 265 nm.

All measurements were performed using the same HPLC apparatus as for determination of phenolics.

Statistical analysis

Two-way repeated-measures ANOVA (REPEATED/PROFILE option in the SAS GLM procedure; SAS Institute, 2004) was employed to test the differences in the photosynthetic parameters measured on the first and the last (ninth) day of experiment (within-subject factor) in plants exposed to different PAR and UV-B regimes (between-subject factors). The profile analysis tested three hypotheses: the 'parallelism' (similarity in shape of the response curves), 'levels' (significance of UV-B and PAR effects) and 'flatness' (significance of a trait change during time). To identify specific time intervals in which significant treatment effects occurred we performed individual ANOVAs on each of the contrasts of the within-subject factor (duration of exposure to different treatments).

Two-way ANOVA was used to reveal the effects of UV-B radiation, PAR and their interactions on the pigment contents and ratios in the green leaf portions of *P. coleoides* plants.

The significance of the effects of tissue type (green and white tissues), UV-B radiation and different PAR regimes as well as their interaction on phenolics content, reduced ascorbate content and activities of APX and POD were tested for each functional group by the three-way nested ANOVA without replication. Since green and white segments were pooled from the leaves of the same plant, the plant was nested in "tissue type × UV-B × PAR" interaction and obtained mean squares (MS) were used as MSerror for calculation of F

values, i.e., mean squares of main and interaction effects were divided with this MSerror (SAS GLM procedure; SAS Institute, 2004).

To distinguish only the UV-B effects on photosynthesis, pigment contents and chloroplast ultarstructure Mann-Whitney U test was used on group of plants with and without UV-B addition under the same PAR. Tukey's post hoc test was used to test for significant differences in phenolics and antioxidants among different treatment groups. Mann-Whitney U test and Tukey's post hoc test were conducted with IBM SPSS statistics software (Version 20.0, SPSS Inc., Chicago, USA). Significance threshold value was set at 0.05.

Results

Effect of UV-B radiation on chlorophyll fluorescence and gas exchange parameters under LL and HL

UV-B radiation significantly increased the CO_2 assimilation rate (*A*) of *P. coleoides* plants at LL after 4 h of exposure to 0.90 W m^{-2} UV-B radiation (Table 2). Furthermore, the enhanced CO_2 assimilation was accompanied by a three-fold increase in stomatal conductance (g_s) and an increased internal CO_2 concentration (c_i) compared to plants grown under LL without UV-B radiation. On the ninth day under LL+UV-B, g_s remained four-fold higher than in LL plants, whereas stimulation of *A* and c_i was less pronounced compared to the first day of the experiment (Table 2). At HL, the UV-B supplementation on the first day resulted in significantly increased g_s and slightly increased *A*, without changes in c_i compared with the HL regime (Table 2). The simultaneously determined PS II efficiency was significantly increased by UV-B radiation only under LL on the first day (Table 2; for significance values of "UV-B", "PAR" and "days" effects and interactions see Supporting Information, Table S1).

The non-photochemical quenching (NPQ) was not affected by UV-B radiation at LL. However, at HL, NPQ doubled compared to LL. Significantly increased NPQ was observed only after nine days at HL+UV-B compared to HL (Table 2; for significance values of "PAR × UV-B" interactions see Supporting Information, Table S1).

Table 2.

Effect of UV-B radiation on photosynthetic pigments under LL and HL

UV-B supplementation did not significantly affect the photosynthetic pigment contents, although a decreasing trend was observed; however, slightly increased levels of zeaxanthin

and antheraxanthin in the HL+UV-B treatment compared to the HL treatment were observed (Table 3). By contrast, PAR had a significant effect on the chlorophyll *a*, chlorophyll *b*, neoxanthin and lutein contents (significance values of "PAR" effects and post hoc analysis see Supporting Information, Table S2). The levels of antheraxanthin and zeaxanthin were below the detection limit under the LL treatment (Table 3).

Table 3.

Effect of UV-B radiation on chloroplast ultrastructure under HL

The green and white leaf tissues of *P. coleoides* plants showed markedly different subplastid organisation. Within the green leaf tissue, the ultrastructural examination showed that the sectioned chloroplasts contained a well-developed thylakoid system with distinct grana stacks, well-defined plastoglobuli and starch grains. By contrast, the plastids in the white leaf tissue lacked thylakoid membranes and starch grains (Fig. 1). These plastids accumulated numerous membrane vesicles of varying sizes and plastoglobuli in the interior soluble region. Therefore, only the green leaf sections were further analysed, and comparisons between plants exposed to HL and HL+UV-B radiation regime were performed (Table 4). The UV-B radiation increased the surface area of the stroma (1.4 times; $P \leq 0.001$) and doubled the number of plastoglobuli ($P \leq 0.001$). On the other hand, the UV-B irradiance had no effect on the thylakoids and starch abundance.

Fig. 1.

Table 4.

Induction of flavonoid pathway upon UV-B radiation under LL and HL

The profiles of the methanol soluble phenolic compounds in the white and green leaf portions of *P. coleoides* plants exposed to UV-B radiation and different PAR analysed by HPLC illustrated that the major soluble phenylpropanoids in *P. coleoides* plants were derivatives of rosmarinic (RA) and caffeic acid (CA) (Fig. 2). In addition, four flavonoids, catechin (Cat), epicatechin (ECat), apigenin (Ap) and cyanidin (Cy), were identified in the form of glycosides. Our analysis revealed about five times higher contents of hydroxybenzoic acids (HBAs), hydroxycinnamic acids (HCAs), ECat and Cat in the green tissue compared to white tissue at both PAR levels (Fig. 2, significant "tissue" effects in Supporting Information, Table S3).

Fig. 2.

The most striking effect of the UV-B radiation on the phenolic content in the whole leaves was the increased accumulation of apigenin and cyanidin glycosides, especially in the white tissue (Fig. 2; significant UV-B-effects and "tissue × UV-B" in Supporting Information Table S3). The first visible signs of anthocyanin accumulation were observed in the leaves of *P. coleoides* plants after four days of exposure to UV-B radiation and were more noticeable under HL compared to LL. After nine days, the white leaf portions expressed intense pink coloration (Supporting Information Fig. S2). The UV-B radiation induced a three-fold increase in the Ap concentration in both green and white leaf tissues, and the highest amount was determined in the white tissue under the LL+UV-B treatment (Fig. 2).

The HBA and CA concentrations were significantly increased by UV-B radiation only under the HL treatment by 60% and 80% in the green leaf portions, respectively (Fig. 2 and significant "UV-B × PAR" interaction, Supporting Information, Table S3). The

concentrations of RA, CA, Cat and ECat were decreased under HL compared to LL in the green leaf portions (Fig. 2, Table S3).

Protein carbonylation

To determine whether UV-B radiation imposed oxidative stress, we compared the levels of carbonylated proteins in the plants exposed to HL and HL+UV-B. The content of protein carbonyls (determined spectrophotometrically using 2,4-dinitrophenylhydrazine) was higher in green tissue compared to white tissue at high PAR (Table 5). The addition of UV-B radiation did not increase the level of protein carbonyls in the whole leaf.

Table 5.

Effect of UV-B radiation on antioxidants under LL and HL

The concentration of reduced ascorbate was three times higher in the green leaf portion at HL compared to LL (Fig. 3) and was accompanied by increased APX activity. Furthermore, 2.5-fold higher POD activity was measured in the whole leaf at HL compared to LL. However, UV-B radiation significantly reduced the Asc concentration at HL in the green leaf tissue. In addition, under the HL+UV-B regime, POD activity decreased in both tissues compared to HL, whereas APX activity did not change significantly (Fig. 3). At LL, UV-B radiation induced a significant decrease in APX activity only in the white leaf tissue, whereas POD activity decreased in the green leaf tissue. In addition to guaiacol, peroxidase substrate affinity was tested over a range of phenolics that are naturally present in the leaves. Peroxidases extracted from green and white leaf tissues of *P. coleoides* could efficiently scavenge H_2O_2 using the main phenolics present in the leaves (CA, Cat, ECat) as electron donors (data not shown).

The statistical analysis results confirming the effects of PAR on Asc, APX and POD and the different effects of UV-B radiation under different background light in the case of Asc and POD are shown in Supporting Information, Table S4.

Fig. 3.

Discussion

UV-B effects on photosynthesis

In this study, we exploited the variegation in *P. coleoides* to identify the photosynthetically mediated effects of UV-B radiation on leaves. White leaf tissue in variegated plants acts as an additional sink of assimilates from the photosynthetically active part of the leaf. Aluru and colleagues (2009) used variegated *Arabidopsis immutans* mutants to study the nature of "sink metabolism" in white leaf tissues.

Under our experimental conditions, supplemental realistic UV-B radiation was beneficial for sustaining the maximal photosynthetic rates in variegated *P. coleoides* plants, especially at LL (Table 2). To our knowledge, the stimulation of photosynthesis under realistic UV-B radiation has not been observed thus far. Most studies report the deleterious effects of above-ambient UV-B levels on photosynthesis, either by using supplemental UV-B radiation in greenhouses or growth chambers (Nogués *et al.* 1998, 1999; Kakani 2003; Ranjbarfordoei, Samson & Van Damme 2011) or by conducting experiments under natural conditions with relatively high solar UV-B radiation (i.e., high altitudes, polar regions) (Albert *et al.* 2008, 2011; Ruhland *et al.* 2008; Berli *et al.* 2013). On the other hand, the impact of lower doses of UV-B radiation on photosynthesis under realistic, field conditions is assumed to be minimal (Ballaré *et al.* 2011; Hideg, Jansen & Strid 2013; Müller *et al.* 2013),

394 although the stimulated growth of several species was reported (Kumagai *et al.*
395 2001, Müller *et al.* 2013; Yu *et al.* 2013).

396 The observed enhancement of CO_2 assimilation in variegated *P. coleoides* plants
397 under LL+UV-B conditions on the first day may be explained by the rapid UV-B response of
398 stomata overcoming the stomatal limitation of photosynthesis, whereas a significant effect
399 was not observed at HL. Reports on UV-B impacts on stomatal conductance are inconsistent,
400 which could be explained by various PAR/UV-B ratios, the time of exposure (Jansen & van
401 der Noort 2000) and species- or cultivar-specific UV-B responses (Klem *et al.* 2012; Gitz,
402 Britz & Sullivan 2013).

403 *Photosynthetic pigments and chloroplast ultrastructure*

404 Our results, which showed no significant influence of UV-B radiation on chlorophyll
405 content, are consistent with previous studies that have observed either no effect
406 (Ranjbarfordoei, Samson & Van Damme 2011; Yi *et al.* 2013) or a reduction of
407 photosynthetic pigments (Surabhi, Reddy & Singh 2009; Hu *et al.* 2013). However, under the
408 HL treatment, UV-B radiation slightly increased the levels of antheraxanthin and zeaxanthin,
409 which implicated a higher level of de-epoxidation. Similar results were obtained in beech
410 leaves following exposure to ambient and to enhanced UV-B doses (Laposi, Veres &
411 Meszaros 2008).

412 The comparison of chloroplast ultrastructure from plants exposed to HL and HL+UV-
413 B for nine days showed doubled plastoglobuli size without a decrease in starch content (Table
414 4). It has been considered that under high light, lipid membrane components as well as the
415 degradation products of electron transport chain components and pigments are partially
416 conserved in plastoglobuli (Ladygin 2004; Lichtenthaler 2007). Although the thylakoid
417 membrane structure was not altered by UV-B exposure under HL, the response of
418 photosynthetic pigments might be related to plastoglobuli formations (Table 3 and 4). Similar

419 results regarding plastoglobuli accumulation triggered by a comparable intensity of UV-B
420 radiation were reported for super-high-yield hybrid rice, which was associated with the
421 decreased activities of photophosphorylation and key enzymes in carbon fixation (Yu *et al*.
422 2013).

423 *UV-B induction of flavonoids*

424 A hallmark of UV-B induced changes in plant metabolism is the induction of
425 phenylpropanoid and flavonoid pathways (Brown *et al*. 2005, Götz *et al*. 2010, Agati *et al*.
426 2009, Agati & Tattini 2010). In our experiments, this was demonstrated by the accumulation
427 of apigenin and cyanidin glycosides, which increased in both leaf tissues of *P. coleoides* (Fig.
428 2). Apigenin and cyanidin glycosides and caffeic acid derivatives can serve as effective UV-
429 B-shielding compounds due to their strong absorbance in this spectral range. The efficiency
430 of flavonoids and hydroxycinnamic derivatives as UV-B-screening pigments has been shown
431 in a number of species (Rueber, Bornman & Weissenböck.1996; Ibdah *et al*. 2002; Götz *et al*.
432 2010). UV absorbing compounds are mainly localized in the epidermal layer (Cerovic *et al*.
433 2002) although flavonoids were detected in the mesophyll layer as well (Agati *et al*. 2009).

434 One can assume different UV-B radiation penetration in green and non-
435 chlorophyllous tissue due to absence of chlorophyll, thus implying a different effect on
436 phenylpropanoid metabolism in these two types of tissues. Chlorophyll absorbs in UV
437 spectral range to a certain level (Bilger *et al*. 1997; Cerovic *et al*. 2002) and may
438 consequently partly attenuate UV-B radiation in green tissue. However, specifically UV-B-
439 induced flavonoids, apigenin and cyanidin, were increased to the similar level in both tissues
440 under all conditions except cyanidin at HL+UV-B which was more accumulated in white
441 tissue (Fig 2). The accumulation of anthocyanins was observed in the abaxial and adaxial leaf
442 epidermis. Also, we obtained the specific UV-B induced increase of hydroxybenzoic acids
443 and caffeic acid derivatives in green tissue under HL. No UV-B-induced changes of other

444 phenolics (except apigenin and cyanidin) were observed in white sectors irrespective to
445 background light. Taken together, our results imply that the presence of chlorophyll and
446 higher basal level of phenolics (UV absorbers) in green tissue did not reduce the UV-B effect.
447 The accumulation of UV-B-provoked flavonoids in white leaf tissue supports the
448 hypothesis that UV-B radiation is a specific signal for flavonoid pathway not related to
449 photosynthetic activity. However, approximately five-fold higher content of almost all
450 phenolic subclasses in the green leaf tissue indicates their relationship with photosynthetic
451 activity. Up to 20% photoassimilates flow to phenylpropanoid pathway (Jensen, 1986), yet
452 the interaction between photosythesis and phenolic metabolism is not clear (Fritz et al. 2006).
453 More extensive research is needed to elucidate a possible link between increased
454 photosynthesis and stimulation of flavonoid metabolism.
455 *Antioxidative role of induced phenolics: relationship with H_2O_2 scavenging systems*
456 There is strong evidence from previous studies favouring the antioxidative function of
457 flavonoids in photoprotection rather than just sun protection in leaf epidermal cells (Neill *et*
458 *al.* 2002; Agati *et al.* 2009; Agati & Tattini 2010; Hernández *et al.* 2009). Although the
459 concentrations of caffeic acid, rosmarinic acid, catechin and epicatechin (all with ortho-
460 dihydroxy B-ring substitution pattern) showed little differences with respect to UV-B
461 radiation, they likely acted as a constitutive antioxidative "pool", as supported by the
462 preferential distribution in the green tissue. In addition, the total concentration of
463 phenylpropanoids and catechins in *P. coleoides* leaves was 20 to 40 times higher than the
464 ascorbate concentration.
465 The increased ascorbate concentration and up-regulation of both APX and POD in the
466 photosynthetically active tissue indicated a provoked antioxidative response to accumulating
467 oxidative loads under high light intensity (Fig. 4), as has been previously shown (Gechev *et*
468 *al*. 2003; Fryer *et al.* 2003; Heyneke *et al.* 2013; Szechyńska-Hebda & Karpiński 2013).

Accordingly, the higher level of carbonylated proteins in green compared to white tissue (Table 5) confirmed that photosynthesis was the main source of ROS. The increase in PODs under HL, as well as their preferential induction in the green leaf tissue, was correlated with decreased concentrations of CA, RA, Cat and ECat, which are natural POD substrates (Takahama 2004). The PODs isolated from green and white tissue showed a high affinity for standard CA, RA, Cat and ECat solutions (data not shown). Although the concentrations of ascorbate in *P. coleoides* leaves were significantly lower compared to other plant species, e.g., Arabidopsis (Bartoli *et al.* 2006), it can efficiently scavenge H_2O_2 in both the reaction with APX and through the Asc/phenolics/peroxidase system (Takahama 2004).

The down-regulation of APX and POD and the unchanged level of carbonylated proteins at low UV-B doses under HL confirmed that UV-B radiation did not provoke oxidative stress. Accordingly, recent studies have questioned the concept of UV-B stress in environmental conditions and favoured an overall opinion that UV-B-mediated stress in plants is relatively rare (Ballaré *et al*. 2011; Hideg, Jansen & Strid, 2013).

In summary, our study implicates that the UV-B portion of sunlight is important for the photoprotection of photosynthesis, as shown by the stimulation of CO_2 assimilation and stomatal conductance. We propose that UV-B-induced photoprotection under excess light is based on the stimulation of flavonoid biosynthesis that leads to the accumulation of UV screeners in both tissues. However, high PAR specifically provoked the H_2O_2 scavenging system (Asc, APX, PODs) that is targeted to photosynthetically active tissue. In addition, the phenolic compounds already present at LL in green leaf tissue are sufficient to maintain photosynthesis under excess light and UV-B radiation, whereas in white leaf tissue the UV-B-inducible phenolics are more important. Thus, we showed different responses to high PAR and UV-B radiation in both “source” and “sink” tissues.

Acknowledgements

This work was supported by the Ministry of Education, Science and Technological Development of the Republic of Serbia (Project No. III 43010). M.V. wishes to acknowledge the support of COST Action FA0906 for approving STSM in Munich during 2011 and 2012. The authors would like to thank Dr. Jelica Lazarevic and Uros Savkovic (Belgrade University) for help with statistical analysis. M.V. wishes to thank Jacqueline Müller (Helmholtz Zentrum München) for her help with preparing the samples for TEM analysis. The authors would like to thank Prof. Umeo Takahama (Kyushu Dental College) for extensive discussion on the whole manuscript.

References

Agati, G., Stefano, G., Biricolti, S. & Tattini, M. (2009) Mesophyll distribution of 'antioxidant' flavonoid glycosides in *Ligustrum vulgare* leaves under contrasting sunlight irradiance. *Annals of Botany* **104,** 853–861.

Agati, G. & Tattini, M. (2010) Multiple functional roles of flavonoids in photoprotection. *New Phytologist* **186**, 786–793.

Albert, K. R., Mikkelsen, T. N. & Ro-Poulsen, H. (2008) Ambient UV-B radiation decreases photosynthesis in high arctic *Vaccinium uliginosum*. *Physiologia Plantarum* **133**, 199–210.

Albert, K. R., Mikkelsen, T. N., Ro-Poulsen, H., Arndal, M. F. & Michelsen, A. (2011) Ambient UV-B radiation reduces PSII performance and net photosynthesis in high Arctic *Salix arctica*. *Environmental and Experimental Botany* **73**, 10–18.

Aluru, M., Zola, J., Foudree, A. & Rodermel, S. (2009) Chloroplast photooxidation-induced transcriptome reprogramming in Arabidopsis *immutans* white leaf sectors. *Plant Physiology* **150**, 904–923.

Asada, K. (2006) Production and scavenging of reactive oxygen species in chloroplasts and their functions. *Plant Physiology* **141,** 391–396.

Baker, N.R. (2008) Chlorophyll fluorescence: a probe of photosynthesis *in vivo. Annual Review of Plant Biology* **59**, 89–113.

Ballaré, C.L., Caldwell, M.M., Flint, S.D., Robinson, S.A. & Bornman, J.F. (2011) Effects of solar ultraviolet radiation on terrestrial ecosystems. Patterns, mechanisms, and interactions with climate change. *Photochemical & Photobiological Sciences* **10**, 226–241.

Bartoli, C.G., Yu, J., Gómez, F., Fernández, L., McIntosh, L. & Foyer, C.H. (2006) Inter-relationships between light and respiration in the control of ascorbic acid synthesis and accumulation in *Arabidopsis thaliana* leaves. *Journal of Experimental Botany* **57,** 1621–1631.

Berli, F.J., Alonso, R., Bressan-Smith, R. & Bottini, R. (2013) UV-B impairs growth and gas exchange in grapevines grown in high altitude. *Physiologia Plantarum* **149,** 127–140.

Bilger, W. & Björkman, O. (1990) Role of the xanthophyll cycle in photoprotection elucidated by measurements of light-induced absorbance changes, fluorescence and photosynthesis in leaves of *Hedera canariensis*. *Photosynthesis Research* **25**, 173–185.

Bilger, W., Veit, M., Schreiber, L. & Schreiber, U. (1997) Measurement of leaf epidermal transmittance of UV radiation by chlorophyll fluorescence. *Physiologia Plantarum* **101,** 754–763.

Bradford, M. (1976) A rapid and sensitive method for the quantitation of microgram quantities of protein utilizing the principle of protein-dye binding. *Analytical Biochemistry* **72**, 248–254.

Brosché, M., Schuler, M.A., Kalbina, I., Connorb, L. & Strid, Å. (2002) Gene regulation by low level UV-B radiation: identification by DNA array analysis. *Photochemical & Photobiological Sciences* **1**, 656–664.

Brosché, M. & Strid, Å. (2003) Molecular events following perception of ultraviolet-B radiation by plants. *Physiologia Plantarum* **117**, 1–10.

Brown, B.A., Cloix, C., Jiang, G.H., Kaiserli, E., Herzyk, P., Kliebenstein, D.J. & Jenkins, G.I. (2005) A UV-B-specific signaling component orchestrates plant UV protection. *Proceedings of the National Academy of Sciences of the United States of America* **102**, 18225–18230.

Caldwell, M.M. (1971) Solar ultraviolet radiation and the growth and development of higher plants. In: *Photophysiology* (ed. A.C., Giese), Volume 6 pp. 131–177. Academic Press, New York.

552 Caldwell, M.M., Bornman, J.F., Ballaré, C.L., Flint, S.D. & Kulandaivelu, G. (2007)
553 Terrestrial ecosystems, increased solar ultraviolet radiation, and interactions with other
554 climate change factors. *Photochemical & Photobiological Sciences* **6**, 252–266.
555 Cerovic, Z.G., Ounis, A., Cartelat, A., Latouche, G., Goulas, Y., Meyer, S. & Moya, I. (2002)
556 The use of chlorophyll fluorescence excitation spectra for the non-destructive in situ
557 assessment of UV-absorbing compounds in leaves. *Plant, Cell & Environment* **25**, 1663–
558 1676.
559 Chan, T., Galati, G. & O'Brien, P.J. (1999) Oxygen activation during peroxidase catalysed
560 metabolism of flavones or flavanones. *Chemico-Biological Interactions* **122,** 15–25.
561 Döhring, T., Köfferlein, M., Thiel, S. & Seidlitz, H.K. (1996) Spectral shaping of artificial
562 UV-B irradiation for vegetation stress research. *Journal of Plant Physiology* **148,** 115–119.
563 Fischer, B.B., Hideg, É. & Krieger-Liszkay, A. (2013) Production, detection and signaling of
564 singlet oxygen in photosynthetic organisms. *Antioxidants & Redox Signaling* **18,** 2145–2162.
565 Foyer, C.H. & Shigeoka, S. (2011) Understanding oxidative stress and antioxidant functions
566 to enhance photosynthesis. *Plant Physiology* **155,** 93–100.
567 Fritz, C., Palacios-Rojas, N., Feil, R. & Stitt, M. (2006) Regulation of secondary metabolism
568 by the carbon–nitrogen status in tobacco: nitrate inhibits large sectors of phenylpropanoid
569 metabolism. *The Plant Journal* **46**, 533–548.
570 Fryer, M.J., Ball, L., Oxborough, K., Karpinski, S., Mullineaux, P.M. & Baker, N.R. (2003).
571 Control of ascorbate peroxidase 2 expression by hydrogen peroxide and leaf water status
572 during excess light stress reveals a functional organization of *Arabidopsis* leaves. *The Plant*
573 *Journal* **33**, 691–705.
574 Gechev, T., Willekens, H., Van Montagu, M., Inzé, D., Van Camp, W., Toneva, V. &
575 Minkov I. (2003) Different responses of tobacco antioxidant enzymes to light and chilling
576 stress. *Journal of Plant Physiology* **160**, 509–515.

577 Gitz, D.C., Britz, S.J. & Sullivan, J.H. (2013) Effect of ambient UV-B on stomatal density,
578 conductance and isotope discrimination in four field grown soybean [*Glycine max* (L.) Merr.]
579 isolines. *American Journal of Plant Sciences* **4,** 100–108.
580 Götz, M., Albert, A., Stich, S., Heller, W., Scherb, H., Krins A.,…, Ernst, D. (2010) PAR
581 modulation of the UV-dependent levels of flavonoid metabolites in *Arabidopsis thaliana* (L.)
582 Heynh. leaf rosettes: cumulative effects after a whole vegetative growth period. *Protoplasma*
583 **243,** 95–103.
584 Green, A.E.S., Sawada, T. & Shettle, E.P. (1974). The middle ultraviolet reaching the
585 ground. *Photochemistry and Photobiology* **19**, 251–259.
586 Heijde, M. & Ulm, R. (2012) UV-B photoreceptor-mediated signalling in plants. *Trends in*
587 *Plant Science* **17**, 230–237.
588 Hernández, I., Alegre, L., Van Breusegem, F. & Munné-Bosch, S. (2009) How relevant are
589 flavonoids as antioxidants in plants? *Trends in Plant Science* **141,** 125–132.
590 Hertog, M.G., Hollman, P.C. & Venem, D.P. (1992) Optimization of a quantitative HPLC
591 determination of potentially anticarcinogenic flavonoids in vegetables and fruits. *Journal of*
592 *Agricultural and Food Chemistry* **40,** 1591–1598.
593 Heyneke, E., Luschin-Ebengreuth, N., Krajcer, I., Wolkinger, V., Müller, M. & Zechmann,
594 B. (2013) Dynamic compartment specific changes in glutathione and ascorbate levels in
595 Arabidopsis plants exposed to different light intensities. *BMC Plant Biology* **13**, 104–123.
596 Hideg, É. & Vass, I. (1996) UV-B induced free radical production in plant leaves and isolated
597 thylakoid membranes. *Plant Science* **115,** 251–260.
598 Hideg, É., Jansen, M.A.K. & Strid, Å. (2013) UV-B exposure, ROS, and stress: inseparable
599 companions or loosely linked associates? *Trends in Plant Science* **18,** 107–115.

Hu, Z., Li, H., Chen, S. & Yang, Y. (2013) Chlorophyll content and photosystem II efficiency in soybean exposed to supplemental ultraviolet-B radiation. *Photosynthetica* **51**, 151–157.

Ibdah, M., Krins, A., Seidlitz, H.K., Heller, W., Strack, D. & Vogt, T. (2002) Spectral dependence of flavonol and betacyanin accumulation in *Mesembryanthemum crystallinum* under enhanced ultraviolet radiation. *Plant, Cell & Environment* **25**, 1145–1154.

Jansen, M.A.K. & van den Noort, R.E. (2000) Ultraviolet-B radiation induces complex alterations in stomatal behaviour. *Physiologia Plantarum* **110**, 189–194.

Jansen, M.A.K., Gaba, V. & Greenberg, B.M. (1998) Higher plants and UV-B radiation: balancing damage, repair and acclimation. *Trends in Plant Science* **3**, 131–135.

Jansen, M.A.K., Hideg, É. & Lidon, F.J.C. (2012) UV-B radiation: "When does the stressor cause stress?" *Emirates Journal of Food and Agriculture* **24** (6).

Jenkins, G.I. (2009) Signal transduction in responses to UV-B Radiation. *Annual Review of Plant Biology* **60**, 407–431.

Jensen, R.A. (1986) The shikimate/arogenate pathway: link between carbohydrate metabolism and secondary metabolism. *Physiologia Plantarum* **66,** 164–168.

Jiao, Y., Lau, O.S. & Deng, X.W. (2007) Light-regulated transcriptional networks in higher plants. *Nature Reviews Genetics* **8,** 217–230.

Kakani, V.G., Reddy, K.R., Zhao, D. & Sailaja, K. (2003) Field crop responses to ultraviolet-B radiation: a review. *Agricultural and Forest Meteorology* **20**, 191–218.

Klem, K., Ač, A., Holub, P., Kovác, D., Špunda, V., Robson, T. M. & Urban, O. (2012) Interactive effects of PAR and UV radiation on the physiology, morphology and leaf optical properties of two barley varieties. *Environmental and Experimental Botany* **75**, 52–64.

Kumagai, T., Hidema, J., Kang, H-S. & Sato, T. (2001) Effects of supplemental UV-B radiation on the growth and yield of two cultivars of Japanese lowland rice (*Oryza sativa* L.)

under the field in a cool rice-growing region of Japan. *Agriculture, Ecosystems & Environment* **83,** 201–208.

Ladygin, V.G. (2004) Photosystem damage and spatial architecture of thylakoids in chloroplasts of pea chlorophyll mutants. *Biology Bulletin of the Russian Academy of Sciences* **31**, 268–276.

Laposi, R., Veres, S. & Meszaros, I. (2008) Ecophysiological investigation of UV-B tolerance of beech saplings (*Fagus sylvatica* L.). *Acta Silvatica & Lingaria Hungarica* **4,** 7–16.

Lichtenthaler, H.K. (2007) Biosynthesis, accumulation and emission of carotenoids, alpha-tocopherol, plastoquinone, and isoprene in leaves under high photosynthetic irradiance. *Photosynthesis Research* **92,** 163–179.

Lidon, F.J.C., Reboredo, F.H., Leitã, A.E., Silva, M.M.A., Duarte, P. & Ramalho, J.C. (2012) Impact of UV-B radiation on photosynthesis – an overview. *Emirates Journal of Food and Agriculture* **24**, 546–556.

Morina, F., Jovanovic, Lj., Mojovic, M., Vidovic, M., Pankovic, D. & Veljovic Jovanovic, S. (2010) Zinc-induced oxidative stress in *Verbascum thapsus* is caused by an accumulation of reactive oxygen species and quinhydrone in the cell wall. *Physiologia Plantarum* **140**, 209–224.

Müller, V., Albert, A., Winkler, J.B., Lankes, C., Noga, G. & Hunsche, M. (2013) Ecologically relevant UV-B dose combined with high PAR intensity distinctly affect plant growth and accumulation of secondary metabolites in leaves of *Centella asiatica* L. Urban. *Journal of Photochemistry and Photobiology B: Biology* **127,** 161–169.

Nakano, Y. & Asada, K. (1981) Hydrogen peroxide is scavenged by ascorbate-specific peroxidase in spinach chloroplasts. *Plant & Cell Physiology* **22**, 867–880.

649 Neill, S.G., Gould, K.S., Kilmartin, P.A., Mitchell, K.A. & Markham, K.R. (2002)
650 Antioxidant activity of red versus green leaves in *Elatostema rugosum*. *Plant, Cell &*
651 *Environment* **25**, 539–547.
652 Nogues, S., Allen, D.J., Morison, J.I. & Baker, N.R. (1998) Ultraviolet-B radiation effects on
653 water relations, leaf development, and photosynthesis in droughted pea plants. *Plant*
654 *Physiology* **117**, 173–181.
655 Nogues, S., Allen, D.J., Morison, J.I. & Baker, N.R. (1999) Characterization of stomatal
656 closure caused by ultraviolet-B radiation. *Plant Physiology* **121**, 489–496.
657 Polle, A., Chakrabarti, K., Schurmann, W. & Rennenberg, H. (1990) Composition and
658 properties of hydrogen peroxide decomposing systems in extracellular and total extracts from
659 needles of Norway spruce (*Picea abies* L., Karst.). *Plant Physiology* **94**, 312–319.
660 Ranjbarfordoei, A., Samson, R. & Van Damme, P. (2011) Photosynthesis performance in
661 sweet almond [*Prunus dulcis* (Mill) D. Webb] exposed to supplemental UV-B radiation.
662 *Photosynthetica* **49**, 107–111.
663 Rice-Evans, C.A., Miller, N.J. & Papanga, G. (1996) Structure-antioxidant relationships of
664 flavonoids and phenolic acids. *Free Radical Biology & Medicine* **20,** 933–956.
665 Rueber, S., Bornman, J. F. & Weissenböck, G. (1996) Phenylpropanoid compounds in
666 primary leaves of rye (*Secale cereale*) - light regulation of their biosynthesis and possible role
667 in UV-B protection. *Physiologia Plantarum* **97**, 160–168.
668 Ruhland, C.T., Xiong, F.S., Clark, W. D. & Day, T.A. (2005) The influence of ultraviolet
669 radiation on growth, hydroxycinnamc acids and flavonoids of *Deschampsia antarctica* during
670 springtime ozone depletion in Antarctica. *Photochemistry and Photobiology* **81**, 1086–1093.
671 Surabhi, G., Reddy, K. & Singh, S. (2009) Photosynthesis, fluorescence, shoot biomass and
672 seed weight responses of three cowpea (*Vigna unguiculata* [L.] Walp) cultivars with

673 contrasting sensitivity to UV-B radiation. *Environmental and Experimental Botany* **66**, 160–
674 171.
675 Szechyńska-Hebda, M. & Karpiński, S. (2013) Light intensity-dependent retrograde
676 signalling in higher plants. *Journal of Plant Physiology* **170**, 1501–1516.
677 Takahama, U. & Oniki, T. (1997) A peroxidase/phenolics/ascorbate system can scavenge
678 hydrogen peroxide in plant cells. *Physiologia Plantarum* **101**, 845–852.
679 Takahama, U. (2004) Oxidation of vacuolar and apoplastic phenolic substrates by peroxidase:
680 physiological significance of the oxidation reactions. *Phytochemistry Reviews* **3**, 207–219.
681 Tausz, M., Kranner, I. & Grill, D. (1998) Simultaneous determination of ascorbic acid and
682 dehydroascorbic acid in plant materials by high performance liquid chromatography.
683 *Phytochemical Analysis* **2**, 69–72.
684 Teramura, A.H. & Sullivan, J.H. (1994) Effects of UV-B radiation on photosynthesis and
685 growth of terrestrial plants. *Photosynthesis Research* **39**, 463–473.
686 Thiel, S., Döhring, T., Köfferlein, M., Kosak, A., Martin, P. & Seidlitz, H.K. (1996) A
687 phytotron for plant stress research: how far can artificial lighting compare to natural sunlight?
688 *Journal of Plant Physiology* **148**, 456–463.
689 Thordal-Christensen, H., Zhang, Z., Wei, Y. & Collinge, D.B. (1997) Subcellular localization
690 of H_2O_2 in plants. H_2O_2 accumulation in papillae and hypersensitive response during the
691 barley-powdery mildew interaction. *The Plant Journal* **11**, 1187–1194.
692 Wildi, B. & Lütz, C. (1996) Antioxidant composition of selected high alpine plant species
693 from different altitudes. *Plant, Cell & Environment* **19**, 138–146.
694 Xu, C., Natarajan, S. & Sullivan, J.H. (2008) Impact of solar ultraviolet-B radiation on the
695 antioxidant defense system in soybean lines differing in flavonoid contents *Environmental*
696 *and Experimental Botany* **63**, 39–48.

Yu, G.H., Li, W., Yuan, Z.Y., Cui, H.Y., Lv, C.G, Gao, Z.P., Han, B., Gong, Y.Z. & Chen, G.X. (2013) The effects of enhanced UV-B radiation on photosynthetic and biochemical activities in super-high-yield hybrid rice Liangyoupeijiu at the reproductive stage. *Photosynthetica* **51**, 33–44.

Tables:

Table 1. Irradiance and exposure values of the different radiation regimes. Biologically effective UV-B data, indicated by index BE, are weighted after Green, Sawada & Shettle (1974) according to measurements of Caldwell (1971), normalised at 300 nm. The PAR irradiance used in the low PAR treatment (LL: 395 µmol m^{-2} s^{-1}) corresponded to the greenhouse conditions. The irradiation regime of the high PAR treatment (HL: 1350 µmol m^{-2} s^{-1} PAR) and 0.90 W m^{-2} UV-B radiation values can be compared to sunny spring conditions in mid-northern latitudes. The day/night cycle was 12 h/12 h. The light intensity switched on gradually during the first two hours at the beginning and switched off during the last two hours at the end of the day. UV-B radiation started 1 h after onset of PAR and lasted for ten hours.

Parameters	Low PAR treatment (LL)		High PAR treatment (HL)	
	LL	LL+UV-B	HL	HL+UV-B
PAR (µmol m^{-2} s^{-1})	395	395	1350	1350
UV-A irradiance, (W m^{-2})	7.0	10.0	20.0	28.0
UV-B irradiance, (W m^{-2})	0	0.90	0	0.90
Biologically effective UV-B irradiance, (mW m^{-2})$_{BE}$	0	215.0	0	215.0
Daily PAR radiant exposure (mol m^{-2} d^{-1})	14.2	14.2	14.2	48.8
Daily UV-A radiant exposure (kJ m^{-2} d^{-1})	252	360	711	1008
Daily UV-B radiant exposure (kJ m^{-2} d^{-1})	0	29.3	0	29.3
Daily UV-B radiant exposure (kJ m^{-2} d^{-1})$_{BE}$	0	7.0	0	7.0
Duration (days)	9	9	9	9

Table 2. UV-B effects on photosynthetic parameters in *P. coleoides* plants exposed to four radiation regimes (1) 395 µmol m^{-2} s^{-1} PAR (LL); (2) LL+UV-B (UV-B: 0.90 W m^{-2}); (3) 1350 µmol m^{-2} s^{-1} PAR (HL) and (4) HL+UV-B for nine days. Values represent means ± SE (n = 4). Significant differences between the UV-B treated plants and LL and HL, according to the Mann-Whitney U test, are indicated ($^{*}P < 0.05$). *A*: CO_2 assimilation rate; g_s: stomatal conductance; ETR: electron transfer rate; F_q'/F_m': operating efficiency of PSII, NPQ: non-photochemical quenching, NPQ = $(F_m - F_m') / F_m'$; c_i: CO_2 concentration inside the leaf.

Days of exposure	Photosynthetic parameters	Radiation regime			
		LL	LL+UV-B	HL	HL+UV-B
1st day	*A* (µmol m^{-2} s^{-1})	4.3 ± 0.4	8.6 ± 0.3*	8.6 ± 0.2	10.5 ± 1.0
	g_s (mmol m^{-2} s^{-1})	41.6 ± 6.0	128.9 ± 12.3*	133.7 ± 10.0	184.8 ± 10.1*
	operating efficiency of PSII, F_q'/F_m'	0.58 ± 0.01	0.63 ± 0.01*	0.19 ± 0.02	0.17 ± 0.01
	ETR (µmol m^{-2} s^{-1})	61.2 ± 1.4	66.2 ± 1.0	104.1 ± 12.0	92.7 ± 4.7
	NPQ	0.9 ± 0.1	1.0 ± 0.1	2.1 ± 0.2	2.4 ± 0.1
	c_i, ppm	194.0 ± 27.1	265.9 ± 15.8*	268.4 ± 8.0	282.3 ± 11.5
9th day	*A* (µmol m^{-2} s^{-1})	5.4 ± 0.7	8.1 ± 0.8	11.8 ± 0.7	13.6 ± 1.5
	g_s (mmol m^{-2} s^{-1})	48.2 ± 6.0	198.1 ± 36.7*	169.2 ± 7.1	243.5 ± 26.8
	operating efficiency of PSII, F_q'/F_m'	0.60 ± 0.02	0.61 ± 0.01	0.21 ± 0.01	0.21 ± 0.02
	ETR (µmol m^{-2} s^{-1})	62.8 ± 2.0	63.7 ± 1.5	115.1 ± 3.6	115.4 ± 8.2
	NPQ	0.9 ± 0.1	0.8 ± 0.1	1.8 ± 0.1	2.4 ± 0.2*
	c_i, ppm	201.4 ± 4.3	248.9 ± 36.8	263.0 ± 3.6	283.3 ± 2.1*

Table 3. Contents of chlorophylls and carotenoids (μg g^{-1} FW), pigment ratios (weight ratios) and de-epoxidation index of green leaf portions of *P. coleoides* plants exposed to four radiation regimes (1) 395 μmol m^{-2} s^{-1} PAR (LL); (2) LL+UV-B (UV-B: 0.90 W m^{-2}); (3) 1350 μmol m^{-2} s^{-1} PAR (HL) and (4) HL+UV-B for nine days. Values represent means ± SE (n = 4). No significant differences between the UV-B treated plants and LL and HL according to the Mann-Whitney U test were obtained.

	Radiation regime			
	LL	LL+UV-B	HL	HL+UV-B
Pigment levels				
Chlorophyll *a*	503.8 ± 51.1	439.3 ± 20.5	335.4 ± 11.5	277.6 ± 20.3
Chlorophyll *b*	139.7 ± 12.8	116.4 ± 4.8	90.4 ± 2.5	74.5 ± 5.8
Chlorophyll (*a*+*b*)	643.5 ± 63.8	555.7 ± 25.0	425.8 ± 14.0	352.0 ± 26.0
β-Carotene (C)	27.0 ± 5.9	23.2 ± 3.3	20.8 ± 1.1	16.0 ± 1.3
Lutein (L)	47.7 ± 3.7	40.5 ± 1.8	37.8 ± 0.2	31.5 ± 2.5
Neoxanthin (N)	24.0 ± 2.1	20.5 ± 0.9	17.4 ± 0.2	14.8 ± 1.1
Violaxanthin (V)	29.8 ± 3.3	26.0 ± 2.8	24.3 ± 3.5	16.5 ± 1.1
Antheraxanthin (A)	n.d.	n.d.	5.7 ± 1.2	7.6 ± 0.7
Zeaxanthin (Z)	n.d.	n.d.	6.3 ± 2.2	9.0 ± 0.6
V + A + Z	29.8 ± 3.3	26.0 ± 2.8	36.4 ± 2.0	33.1 ± 2.1
Pigment ratios				
Chlorophyll a/b	3.6 ± 0.1	3.8 ± 0.1	3.7 ± 0.03	3.7 ± 0.1
Chlorophyll (a+b)/ ΣCar [1]	5.0 ± 0.1	5.1 ± 0.2	3.8 ± 0.1	3.7 ± 0.03
De-epoxidation index (Di, %) [2]	-	-	25.2 ± 7.2	38.6 ± 1.3

[1] ΣCar: total carotenoids: (N+L+V+A+Z+ β-Carotene); [2]Di= 100% x (0.5xA+Z)/(V+A+Z). n. d.: not detected

Table 4. Areas of fine structures as the mean percentages with standard errors of the total chloroplasts area in *P. coleoides* plants exposed to 1350 µmol m^{-2} s^{-1} PAR (HL) and HL+ UV-B (UV-B irradiance: 0.90 W m^{-2}). Significant differences between HL+UV-B and HL according to the Mann-Whitney U test are indicated (** $P < 0.01$, *** $P < 0.001$).

Percentages of total chloroplast area	Radiation regime	
	HL	HL+ UV-B
Starch (%)	53.2 ± 3.7	49.5 ± 4.3
Plastoglobules (%)	0.8 ± 0.1	2.0 ± 0.3 ***
Stroma (%)	15.9 ± 1.6	19.3 ± 2.0 **
Thylakoids (%)	30.1 ± 2.8	29.2 ± 3.0

Table 5. Level of carbonylated proteins in the *P. coleoides* leaves exposed to HL (PAR: 1350 µmol m^{-2} s^{-1}) and HL+UV-B (UV-B: 0.90 W m^{-2}) for nine days. Values are shown in nmol of carbonylated proteins per mg of total soluble proteins and represent means ± SE, n = 4.

Leaf tissue	Radiation regime	
	HL	HL+UV-B
Green	159.2 ± 26.1	173.1 ± 19.9
White	51.5 ± 18.3	66.7 ± 11.8

Figure legends:

Fig. 1. TEM micrographs showing the ultrastructure of cells from plants grown under HL (A, B) and HL+UV-B radiation (C, D) from green (A, C) and white (B, D) leaf tissues. Micrographs from green leaf tissues show chloroplasts (C) with large starch grains (St) and numerous plastoglobuli (arrows). The leucoplasts from white leaf tissues contain numerous plastoglobuli (arrows) and vesicles (arrowheads) but no starch grains. CW: cell walls; IS: intercellular spaces; M: mitochondria; N: nuclei; V: vacuoles. Bars = 1 µm. Experimental conditions are described in Table 3.

Fig. 2. Changes in the content of phenolic compounds in the green (grey bars) and white (white bars) leaf tissues of *P. coleoides* plants. Values represent the means of the leaves from four different plants per group. Error bars indicate ± SE, and different letters denote statistically significant differences between the different radiation regimes and different leaf tissues ($P < 0.05$). SyA: syringic acid; HBAs: total hydroxybenzoic acids, CA: caffeic acid, RA: rosmarinic acid; Cat: catechin; ECat: epicatechin; Ap: apigenin; Cy: cyanidin.

Fig. 3. H_2O_2 scavenging system in green (grey bars) and white (white bars) leaf tissues of *P. coleoides* plants under four light regimes. The contents of reduced ascorbate (Asc) in µmol g^{-1}FW; specific activities of ascorbate peroxidase (APX) and guaiacol peroxidase (POD) are shown in U g^{-1}FW Different letters denote statistically significant differences between radiation regimes and leaf tissues ($P < 0.05$). Values represent the means ± SE ($n \geq 4$).

Fig. S1. Simulated irradiance spectra of the four radiation regimes on a linear scale from 300 to 850 nm. The logarithmic scale showing the UV range from 280 to 400 nm is in the right corner.

Fig. S2. The effect of UV-B radiation on *P. coleoides* plants after nine days of treatment. Representative plants are shown.

Supporting information:

Table S1

Table S1. Repeated-measures analysis of variance (profile analysis) on photosynthetic parameters determined on the first and ninth day of the experiment in the leaves of *P. coleoides* plants. Experimental conditions were as described in Table 1. *Dfs* are shown in the brackets (first number represents *Df* of main effects and their interactions and the second number is *Df* of error). Other abbreviations are explained in Table 2.

	A (*Df*: 1; 12)		g_s (*Df*: 1; 12)		Fq'/Fm' (*Df*: 1; 12)		ETR (*Df*: 1; 12)		NPQ (*Df*: 1; 12)		c_i (*Df*: 1; 12)	
Source	*F*	*P* > *F*	*F*	*P* > *F*	*F*	*P* > *F*	*F*	*P* > *F*	*F*	*P* > *F*	*F*	*P* > *F*
Between-subjects												
PAR	**51.37**	**< 0.0001**	**28.47**	**0.0002**	**1383.65**	**< 0.0001**	**166.40**	**< 0.0001**	**228.67**	**< 0.0001**	**10.02**	**0.0081**
UV-B	**17.68**	**0.0012**	**36.55**	**< 0.0001**	0.70	0.4185	0.14	0.7100	**8.40**	**0.0134**	**6.77**	**0.0231**
PAR × UV-B	1.60	0.2302	3.36	0.0917	3.09	0.1040	1.64	0.2239	**7.98**	**0.0153**	2.08	0.1746
Within-subjects	*A* (*Df*: 1; 12)		g_s (*Df*: 1; 12)		Fq'/Fm' (*Df* :1; 12)		ETR (*Df*: 1; 12)		NPQ (*Df*: 1; 12)		c_i (*Df*: 1; 12)	
Day	**17.58**	**0.0012**	**5.87**	**0.0321**	2.93	0.1124	3.41	0.0898	1.76	0.2094	0.12	0.7330
Day × PAR	**12.52**	**0.0041**	0.06	0.8175	2.84	0.1180	3.38	0.0907	0.05	0.8192	0.02	0.8982
Day × UV-B	0.90	0.3620	1.49	0.2460	0.24	0.6350	0.17	0.6867	0.36	0.5621	0.19	0.6698
Day × PAR × UV-B	1.01	0.3340	0.32	0.5819	2.76	0.1224	0.74	0.4058	1.86	0.1974	0.57	0.4655

Table S2

Table S2. Two-way ANOVA results for the effects of UV-B radiation exposure (0.9 W m^{-2}) and two PAR intensities (LL: 395 µmol m^{-2} s^{-1} and HL: 1350 µmol m^{-2} s^{-1}) and their interactions on the pigment contents and ratios in the leaves of *P. coleoides* plants. Experimental conditions were the same as in Table 1. *Dfs* are shown in the brackets (first number represents *Df* of main effects and their interactions and the second number is *Df* of error). Other abbreviations are explained in Table 3.

Trait	Source of variation	*F*	*P* > *F*	Trait	Source of variation	*F*	*P* > *F*
Chl a	UV-B	2.96	0.1108	**β-Carotene**	UV-B	1.77	0.2086
(*Df*=1;16)	**PAR**	**20.84**	**0.0006**	(*Df*=1;16)	PAR	2.46	0.1427
	UV-B × PAR	0.03	0.8731		UV-B × PAR	0.04	0.8485
Chl b	UV-B	4.58	0.0536	**Neoxanthin**	UV-B	4.49	0.0557
(*Df*=1;16)	**PAR**	**26.95**	**0.0002**	(*Df*=1;16)	**PAR**	**17.91**	**0.0012**
	UV-B × PAR	0.16	0.6918		UV-B × PAR	0.14	0.7160
Chl (a+b)	UV-B	2.73	0.1244	**Lutein**	**UV-B**	**6.84**	**0.0226**
(*Df*=1;16)	PAR	1.81	0.2035	(*Df*=1;16)	**PAR**	**13.69**	**0.0030**
	UV-B × PAR	0.02	0.8989		UV-B × PAR	0.12	0.7306
Chl (a/b)	UV-B	3.12	0.1025	**Violaxanthin**	UV-B	3.81	0.0745
(*Df*=1;16)	PAR	0.21	0.6572	(*Df*=1;16)	PAR	4.28	0.0608
	UV-B × PAR	1.92	0.1901		UV-B × PAR	0.20	0.6609
Chl (a+b)/Σcar	UV-B	0.31	0.5872				
	PAR	**123.12**	**< 0.0001**				
	UV-B × PAR	1.83	0.2014				

Table S3

Table S3. Three-way nested ANOVA results for the effects of tissue type (chlorophyllous and non-chlorophyllous tissues), UV-B radiation exposure and two PAR intensities as well as their interaction on the content of phenolic compounds found in the leaves of *P. coleoides* plants. Experimental conditions were as described in Table 1. *Df*s are shown in the brackets (first number represents *Df* of main effects and their interactions and the second number is *Df* of error). HBA: total hydroxybenzoic acid; SyA: syringic acid; CA: caffeic acid, RA: rosmarinic acid; Cat: catechin; ECat: epicatechin; Ap: apigenin; Cy: cyanidin.

Trait	Source of variation	*F*	*P* > *F*	Trait	Source of variation	*F*	*P* > *F*
SyA	**tissue**	**240.61**	**< 0.0001**	**Cat**	**tissue**	**78.36**	**< 0.0001**
(*Df*: 1; 56)	UV-B	0.02	0.8947	(*Df*: 1; 56)	UV-B	1.59	0.2124
	PAR	**5.86**	**0.0188**		PAR	0.57	0.4535
	tissue × UV-B	1.01	0.3192		tissue × UV-B	0.07	0.7969
	tissue × PAR	0.39	0.5367		**tissue × PAR**	**10.05**	**0.0025**
	UV-B × PAR	1.50	0.2252		UV-B × PAR	0.08	0.7777
	tissue × UV-B × PAR	0.33	0.5693		**tissue × UV-B × PAR**	**4.80**	**0.0327**
HBA	**tissue**	**120.17**	**< 0.0001**	**ECat**	**tissue**	**497.66**	**< 0.0001**
(*Df*: 1; 56)	UV-B	3.19	0.0796	(*Df*: 1; 56)	**UV-B**	**5.26**	**0.0255**
	PAR	**44.48**	**< 0.0001**		**PAR**	**40.67**	**< 0.0001**
	tissue × UV-B	0.64	0.4281		**tissue × UV-B**	**11.70**	**0.0012**
	tissue × PAR	2.92	0.0929		tissue × PAR	1.87	0.1774
	UV-B × PAR	**12.10**	**0.0010**		UV-B × PAR	3.28	0.0756
	tissue × UV-B × PAR	0.76	0.3857		tissue × UV-B × PAR	0.15	0.6991
CA	**tissue**	**329.13**	**< 0.0001**	**Ap**	**tissue**	**7.64**	**0.0108**
(*Df*: 1; 56)	UV-B	0.34	0.5616	(*Df*: 1; 56)	**UV-B**	**93.52**	**< 0.0001**
	PAR	**10.61**	**0.0019**		**PAR**	**101.85**	**< 0.0001**
	tissue × UV-B	1.19	0.2793		tissue × UV-B	0.03	0.8549

	tissue × PAR	**5.84**	**0.0190**		**tissue × PAR**	**7.00**	**0.0142**
	UV-B × PAR	**11.01**	**0.0016**		**UV-B × PAR**	**15.46**	**0.0006**
	tissue × UV-B × PAR	**8.04**	**0.0064**		tissue × UV-B × PAR	0.07	0.7976
RA	**tissue**	**493.41**	**< 0.0001**	**Cy**	**tissue**	**21.98**	**< 0.0001**
(*Df*: 1; 56)	**UV-B**	**15.62**	**0.0002**	(*Df*: 1; 56)	**UV-B**	**36.63**	**< 0.0001**
	PAR	**55.17**	**< 0.0001**		**PAR**	**116.13**	**< 0.0001**
	tissue × UV-B	1.88	0.1761		**tissue × UV-B**	**13.80**	**0.0011**
	tissue × PAR	**7.50**	**0.0083**		**tissue × PAR**	**14.08**	**0.0010**
	UV-B × PAR	**10.08**	**0.0024**		**UV-B × PAR**	**16.38**	**0.0005**
	tissue × UV-B × PAR	0.85	0.3597		**tissue × UV-B × PAR**	**8.15**	**0.0087**

Table S4

Table S4. Three-way nested ANOVA results for the effects of tissue type (chlorophyllous and non-chlorophyllous), UV-B radiation exposure (0.90 W m^{-2}) and two PAR intensities (LL: 395 µmol m^{-2} s^{-1} and HL: 1350 µmol m^{-2} s^{-1}) and their interactions on Asc content, APX and POD activities in the leaves of *P. coleoides* plants. Experimental conditions were as described in Table 1. *Df*s are shown in the brackets (first number represents *Df* of main effects and their interactions and the second number is *Df* of error). Other abbreviations are explained in Fig. 4.

Trait	Source of variation	*F*	*P* > *F*	Trait	Source of variation	*F*	*P* > *F*
Asc	**tissue**	**60.36**	**< 0.0001**	**POD**	**tissue**	**33.75**	**< 0.0001**
(*Df* = 1; 40)	UV-B	2.83	0.1004	(*Df* = 1; 52)	**UV-B**	**33.49**	**< 0.0001**
	PAR	**16.02**	**0.0003**		**PAR**	**23.13**	**< 0.0001**
	tissue × UV-B	1.05	0.3122		**tissue × UV-B**	**4.99**	**0.0326**
	tissue × PAR	**24.43**	**< 0.0001**		**tissue × PAR**	**10.10**	**0.0033**
	UV-B × PAR	**11.54**	**0.0016**		**UV-B × PAR**	**6.48**	**0.0159**
	tissue × UV-B × PAR	0.62	0.4369		tissue × UV-B × PAR	0.01	0.9469
APX	tissue	0.01	0.9875				
(*Df* = 1; 40)	**UV-B**	**19.37**	**0.0001**				
	PAR	**4.87**	**0.0357**				
	tissue × UV-B	1.39	0.2483				
	tissue × PAR	2.02	0.1659				
	UV-B × PAR	1.54	0.2248				
	tissue × UV-B × PAR	**11.68**	**0.0020**				

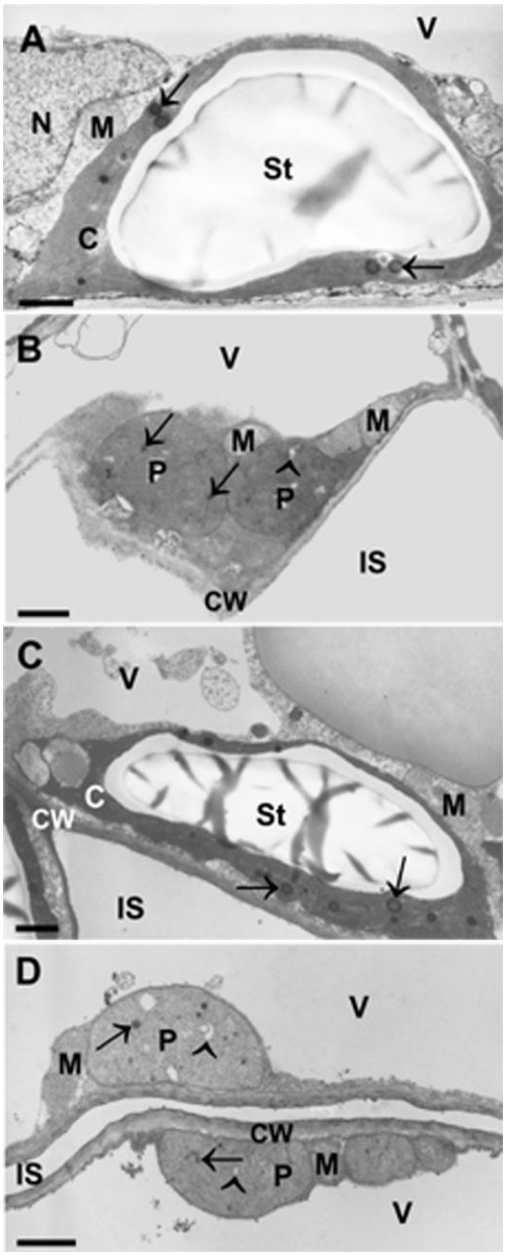

PCE_12471_Fig1